Sensors & Transducers, Vol. 233, Issue 5, May 2019, pp. 1-5

www.sensorsportal.com

Sensors & Transducers

Published by IFSA Publishing, S. L., 2019
http://www.sensorsportal.com

Deterioration of Graphene Nanocoated Optical Taper Saturable Absorber at High Power

[1, *] Meriem KEMEL, [2] Paul MOUCHEL, [1] Georges SEMAAN, [1] Mohamed SALHI, [2] Marc LE FLOHIC, [1] François SANCHEZ

[1] University of Angers, Laboratoire de Photonique d'Angers, E. A. 4464, 2 Boulevard Lavoisier, 49045 Angers, France

[2] Lumibird, 2 rue Paul Sabatier, 22300 Lannion, France

[1] Tel.: +33607058035

[*] E-mail: meriem.kemel@univ-angers.fr

Received: 30 March 2019 /Accepted: 30 April 2019 /Published: 31 May 2019

Abstract: We experimentally investigate the loss of nonlinear transmission of graphene nanocoated optical taper (GNOT) saturable absorber at high input average power. Above a certain threshold of incident average power, the component experiences an irreversible modification of its nonlinear properties. This leads to a permanent deterioration of saturable absorption characteristics of this component. Such behavior is discussed and analyzed.

Keywords: Graphene, Optical tapers, Saturable absorber, Nonlinear optics, Fiber laser.

1. Introduction

Graphene is a two-dimensional (2D) atomic crystal consisting of carbon atoms arranged in a honeycomb-like structure. After monolayer graphene was isolated in 2004 [1], this 2D material has attracted much attention because of its unique properties such as elasticity and mechanical strength [2], impermeable properties to any molecules [3], electrical [4] and thermal [5] conductivity, etc. Thanks to this several properties, graphene is widely studied in numerous domains for several applications like biomedicine [6-7], energy storage [8], electronics [9-10], aerospace [11], etc.

Particularly, we are interested by its saturable absorption characteristics for nonlinear optics applications. Indeed, graphene is widely used in mode-locked fiber lasers in order to produce ultrashort pulses [12-15].

Different methods have been proposed to realize graphene based saturable absorbers (SAs) such as direct deposition of graphene nano-sheet between two fiber connectors [16] or collimators [17], deposition of nano-flakes on a D-shaped side-polished fiber [18] or along the waist of a tapered fiber [19], etc. In our case, we use graphene nanocoated optical tapers (GNOTs). These latter are fabricated by reducing a single mode fiber's diameter to approximately 20 μm over 5 mm waist length. Graphene nano-flakes are then deposited on the taper waist thanks to optical tweezers effect.

While graphene has demonstrated very good saturable absorption properties for low power applications, there are very few results concerning its use in high power fiber lasers [15, 19-20].

In this communication, we point out the deterioration of graphene nonlinear optical properties under high average input power.

2. Methods and Materials

2.1. Fabrication of the GNOT

Graphene based saturable absorber used in this experiment is Graphene nanocoated optical taper (GNOT) which is consisting of optical taper on which graphene nano-flakes are deposited.

The optical tapers are fabricated in Lumibird.

They are consisting of Single Mode Fiber (SMF28), for which the diameter of the tapered part of the fiber is reduced to 20 µm, comprising the core and the optical cladding initially measuring 125 µm for SMF28, along 5 mm of fiber. Fig. 1 presents the taper profile obtained after tapering process.

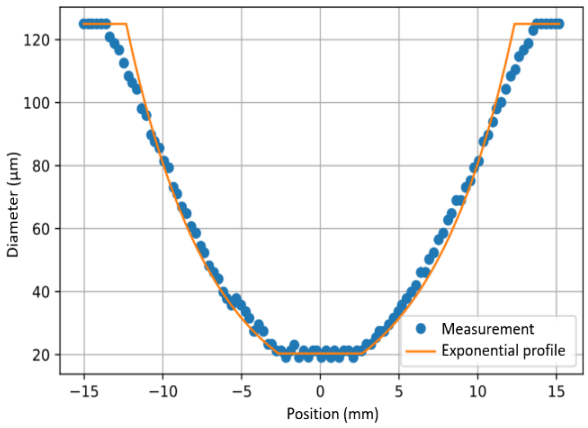

Fig. 1. Measured profile of the fabricated tapers (blue dots) compared to exponential profile (orange curve).

The profile of fabricated tapers is very close to the exponential one used like model to obtain tapers with needed characteristics.

As the dimensions of the fiber in tapered part are significantly reduced, it is needed to be protected to avoid breaking. Indeed, the next step to fabricate the final component is to make graphene deposition on the taper, so this latter is fixed on half glass mount u form and fix the fiber in both sides by UV glue as shown on the Fig. 2.

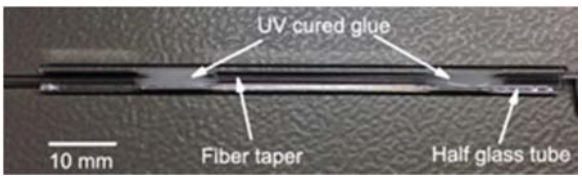

Fig. 2. Photo of taper fixed on a half glass mount.

After protecting the taper, the deposition of graphene will be safe and efficient. The graphene used is in form of nano-flakes in suspension in water (Sigma-Aldrich 799092-50ML) with concentration of 1 $mg \times ml^{-1}$.

The deposition of graphene is made by putting few droplets of this solution on the taper as shown on the Fig. 3. Thanks to optical tweezers effect, graphene nano-flakes are attracted by the taper and they surround all the taper waist while the water is completely evaporated.

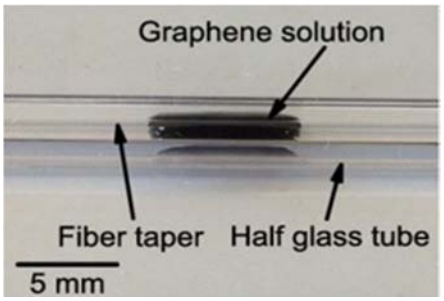

Fig. 3. Photo of the deposited graphene droplet on the taper.

After making sure that the graphene is deposited, graphene nanocoated optical taper is ready to be used as saturable absorber. Fig. 4 presents a photo of the GNOT.

Fig. 4. Photo of the graphene nanocoated optical taper (GNOT).

In the following, this component will be characterized first at low power to study its transmission in function of average input power and then will be characterized at high average input power to study its behavior in conditions of high optical power.

2.2. Characterization of the GNOT

The experimental setup used to measure the nonlinear optical properties of the GNOTs is shown in the Fig. 5. The pulsed laser emits 5 ps pulses at central wavelength of 1562 nm with a repetition rate of 12 MHz. The average power injected in the GNOT is controlled by the variable attenuator. A 50 % -coupler is used to split the beam into two parts. One part goes through a component under study and the second one stands as a reference.

The transmitted power of each arm is measured by using integrating spheres (Thorlabs S145C and S146C respectively).

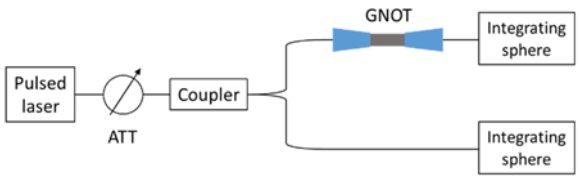

Fig. 5. Experimental setup. ATT: variable attenuator. GNOT: graphene nanocoated optical taper.

Different models of transmission are proposed to fit the experimental transmission curves according to specific cases [13, 21-25]. Here, we propose a general and suitable formula to study our GNOTs. The transmission coefficient T in function of input average power P can be fitted by the equation:

$$T(P) = 1 - \frac{\alpha_s}{1+\left(\frac{P}{P_{sat}}\right)^n} - \alpha_{ns}, \qquad (1)$$

where α_s is the modulation depth of the transmission, α_{ns} is the non saturable (linear) losses and P_{sat} is the saturaion power. The free parameter n has been introduced to take into account the switching region. It permits to control steepness of the slope for a better fitting.

3. Results and Discussion

The transmission measurements of various GNOTs were made and different behaviors were observed.

Fig. 6 presents the transmission of a GNOT for increasing incident average powers.

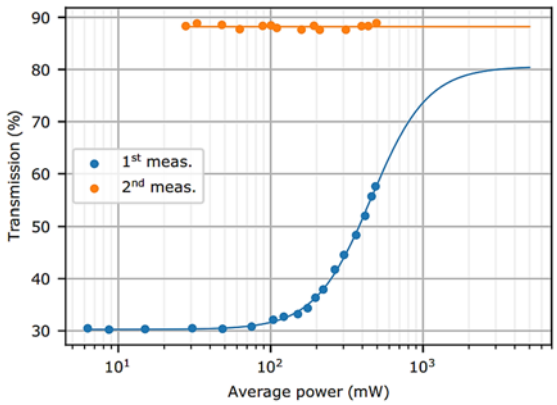

Fig. 6. Transmission of a GNOT. Dots represent measured values and lines are the fitted curves.

For the first measurement (blue dots), the transmission is the usual one for a standard SA: it is low at low powers and then becomes progressively higher for increasing incident power. After this first measurement, the same GNOT has been used to make a second measurement (orange dots). Surprisingly, the resulting transmission is completely independent from incident power and remains nearly constant.

Similar measurements with different GNOTs have been done to confirm this observation.

In order to determine if the incident power causes the deterioration of the components, the stability of the transmission of a GNOT over the time is measured at different incident powers (between 10 mW and 166 mW). These measurements are presented in Fig. 7.

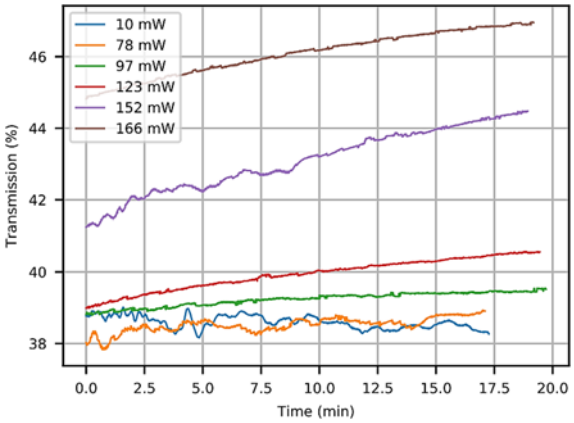

Fig. 7. Transmission evolution of a GNOT over time for different incident average powers. Transmission is measured each second during 20 min.

For the first three measurements corresponding to 10 mW, 78 mW and 97 mW of incident powers, the transmission remains relatively stable over the time as expected for a usual SA. For higher input powers, related to 123 mW, 152 mW and 166 mW, the transmission increases over time and this process is irreversible. By repeating this measurements on few other GNOTs, the damage threshold is determined around 150 mW of incident average power.

We assume that this unusual behavior of transmission is a consequence of a degradation of graphene nano-flakes deposited on the taper. Indeed, due to high power, graphene generates heat. This latter can cause a damage if it is not well dissipated. To verify this hypothesis, a temperature evolution of a GNOT in function of incident average power (between 10 mW and 400 mW) is measured. Fig. 8 presents this evolution which is measured with a thermal camera (Chauvin Arnoux C.A 1882 DiaCAm).

We note that, below damage threshold (determined around 150 mW), the temperature increases up to 124°C. Above 150 mW, the temperature continues to increase before stabilizing at 180 °C. Taking into account the random deposition of graphene nano-flakes on the taper and the low resolution of the camera, it is worth mentioning that this temperature values are most likely averaged over the surface represented by a pixel. Consequently, the peak temperature of the GNOT is certainly higher than values reported here.

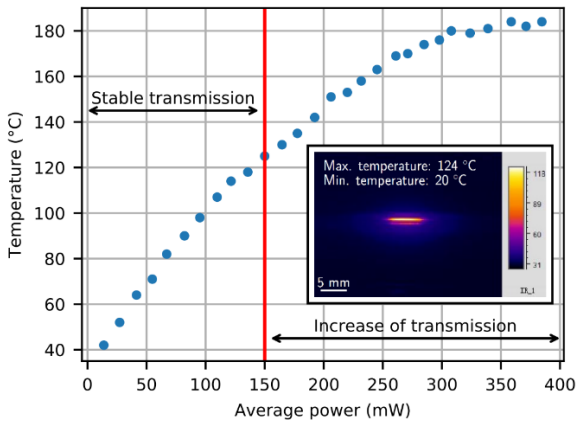

Fig. 8. Temperature evolution of a GNOT in function of incident average power.

In parallel, in previous studies [26-28], it was reported that defects appear on the edges of crystal

Structures of graphene flakes when their temperature reaches 200 °C and in the center of the flakes for temperatures up to 500 °C. In our case, as the flakes are randomly deposited on the taper waist and interact with the evanescent field of clad modes propagating in the taper, the absorption takes place mostly on the edges.

At low temperature (for low average input power), graphene behaves normally as the structure of the flakes is not disrupted by the heat. When the temperature increases, defects appear and the edges stop to absorb the light. For the better understanding of our results, the analysis of the GNOTs (before and after damage) by Raman spectroscopy is needed. Indeed, the damaged GNOTs presented no visible damage and the nano-flakes were still surrounding the taper waist. This implies that the modification of the absorption is a result of structural modification of the graphene rather than of disbonding of graphene from the taper.

4. Conclusion

To conclude, we have reported the deterioration of graphene nanocoated optical taper saturable absorber, while exposed to high incident average power. At low power, the GNOT behaves like a usual saturable absorber. For powers above a certain threshold, determined around 150 mW, the GNOT undergoes an irreversible damage and lose its saturable absorption properties. We assume that this damage is due to the bad cooling of graphene nano-flakes which causes the deterioration of its saturable absorption properties.

References

[1]. K. S. Novoselov, A. K. Geim, S. V. Morozov, D. Jiang, Y. Zhang, S.V. Dubonos, I. V. Grigorieva, A. A. Firsov, Electric Field Effect in Atomically Thin Carbon Films, *Science*, Vol. 306, Issue 5696, 2004, pp. 666-669.

[2]. C. Lee, X. Wei, J. W. Kysar, J. Hone, Measurement of the Elastic Properties and Intrinsic Strength of Monolayer Graphene, *Science*, Vol. 321, Issue 5887, 2008, pp. 385-388.

[3]. J. S. Bunch, S. S. Verbridge, J. S. Alden, A. van der Zande, J. M. Parpia, H. G. Craighead, P. L. McEuen, Impermeable Atomic Membranes from Graphene Sheets, *Nano Letters*, Vol. 8, Issue 8, 2008, pp. 2458-2462.

[4]. I. Meric, M. Y. Han, A. F. Young, B. Ozyilmaz, P. Kim, K. L. Shepard, Current saturation in zero-bandgap, top-gated graphene field-effect transistors, *Nature Nanotechnology*, Vol. 3, Issue 11, 2008, pp. 654-659.

[5]. A. A. Balandin, S. Ghosh, W. Bao, I. Calizo, D. Teweldebrhan, F. Miao, C. N. Lau, Superior Thermal Conductivity of Single-Layer Graphene, *Nano Letters*, Vol. 8, Issue 3, 2008, pp. 902-907.

[6]. Y. Yang, A. M. Asiri, Z. Tang, D. Du, Y. Lin, Graphene based materials for biomedical applications, *Materials Today*, Vol. 16, Issue 10, 2013, pp. 365-373.

[7]. N. Li, Y. Cheng, Q. Song, Z. Jiang, M. Tang, G. Cheng, Graphene meets biology, *Chinese Science Bulletin,* Vol. 59, Issue 13, 2014, pp. 1341-1354.

[8]. D. A. C. Brownson, D. K. Kampouris, C. E. Banks, An overview of graphene in energy production and storage applications, *Journal of Power Sources*, Vol. 196, Issue 11, 2011, pp. 4873-4885.

[9]. F. Schwierz, Graphene transistors, *Nature Nanotechnology*, Vol. 5, Issue 7, 2010, pp. 487-496.

[10]. X. Li, X. Wang, L. Zhang, S. Lee, H. Dai, Chemically derived, ultrasmooth graphene nanoribbon semiconductors, *Science*, Vol. 319, Issue 5867, 2008, pp. 1229-1232.

[11]. P. Kuzhir, N. Volynets, S. Maksimenko, T. Kaplas, Y. Svirko, Multilayered Graphene in K_a-Band: Nanoscale Coating for Aerospace Applications, *Journal of Nanoscience and Nanotechnology*, Vol. 13, Issue 8, 2013, pp. 5864-5867.

[12]. W. D. Tan, C. Y. Su, R. J. Knize, G. Q. Xie, L. J. Li, D. Y. Tang, Mode locking of ceramic Nd:yttrium aluminum garnet with graphene as a saturable absorber, *Applied Physics Letters*, Vol. 96, Issue 3, 2010, p. 031106.

[13]. G. Sobon, J. Sotor, K. Abramski, Passive harmonic mode-locking in Er-doped fiber laser based on graphene saturable absorber with repetition rates scalable to 2.22 GHz, *Applied Physics Letters*, Vol. 100, Issue 16, 2012, p. 161109.

[14]. A. Martinez, Z. Sun, Nanotube and graphene saturable absorbers for fibre lasers, *Nature Photonics*, Vol. 7, Issue 11, 2013, pp. 842-845.

[15]. P. Mouchel, G. Semaan, A. Niang, M. Salhi, M. Le Flohic, F. Sanchez, High power passively mode-locked fiber laser based on graphene nanocoated optical taper, *Applied Physics Letters*, Vol. 111, Issue 3, 2017, p. 031106.

[16]. Y. Meng, A. Niang, K. Guesmi, M. Salhi, F. Sanchez, 1.61 μm high-order passive harmonic mode locking in a fiber laser based on graphene saturable absorber, *Optics Express*, Vol. 22, Issue 24, 2014, pp. 29921-29926.

[17]. Z. C. Luo, W. J. Cao, A. P. Luo, W. C. Xu, Optical deposition of graphene saturable absorber integrated in a fiber laser using a slot collimator for passive mode-locking, *Applied Physics Express*, Vol. 5, Issue 5, 2012, p. 055103.

[18]. T. Chen, C. Liao, D. N. Wang, Y. Wang, Passively mode-locked fiber laser by using monolayer chemical vapor deposition of graphene on D-shaped fiber, *Applied Optics*, Vol. 53, Issue 13, 2014, pp. 2828-2832.

[19]. P. Mouchel, M. Kemel, G. Semaan, M. Salhi, M. Le Flohic, F. Sanchez, Limitations of Graphene nanocoated optical tapers for high power nonlinear applications, *Optical Materials: X*, Vol. 1, 2019, 100003.

[20]. M. Kemel, P. Mouchel, G. Semaan, M. Salhi, M. Le Flohic, F. Sanchez, High-power limitations of Graphene nanocoated optical taper saturable absorbers, in *Proceedings of the Conference on Second International Conference on Optics, Photonics and Lasers (OPAL'19)*, Amsterdam, The Netherlands, 24-26 April 2019, pp. 74-76.

[21]. Q. Bao, H. Zhang, Y. Wang, Z. Ni, Y. Yan, Z. X. Shen, K. P. Loh, D. Y. Tang, Atomic layer graphene as a saturable absorber for ultrafast pulsed lasers, *Advanced Functional Materials*, Vol. 19, Issue 19, 2009, pp. 3077-3083.

[22]. Z. Wang, H. Mu, C. Zhao, Q. Bao, H. Zhang, Harmonic mode-locking and wavelength-tunable Q-switching operation in the graphene-Bi_2Te_3 heterostructure saturable absorber-based fiber laser, *Optical Engineering*, Vol. 55, Issue 8, 2016, p. 081314.

[23]. T. Schibli, E. Thoen, F. Kartner, E. Ippen, Suppression of Q-switched mode locking and break-up into multiple pulses by inverse saturable absorption, *Applied Physics B*, Vol. 70 (S1), 2000, pp. S41-S49.

[24]. C. A. Zaugg, Z. Sun, V. J. Wittwer, D. Popa, S. Milana, T. S. Kulmala, R. S. Sundaram, M. Mangold, O. D. Sieber, M. Golling, Y. Lee, J. H. Ahn, A. C. Ferrari, U. Keller, Ultrafast and widely tuneable vertical-external-cavity surface-emitting laser, mode-locked by a graphene-integrated distributed Bragg reflector, *Optics Express*, Vol. 21, Issue 25, 2013, pp. 31548-31559.

[25]. A. Marini, D. J. Cox, F. J. Garcia de Abajo, Theory of graphene saturable absorption, *Physical Review B*, Vol. 95, Issue 12, 2017, pp. 125408.

[26]. Y. N. Xu, D. Zhan, L. Liu, H. Suo, Z. H. Ni, T. T. Nguyen, C. Zhao, Z. X. Shen, Thermal dynamics of graphene edges investigated by polarized Raman spectroscopy, *ACS Nano*, Vol. 5, Issue 1, 2011, pp. 147-152.

[27]. H. Y. Nan, Z. H. Ni, J. Wang, Z. Zafar, Z. X. Shi, Y. Y. Wang, The thermal stability of graphene in air investigated by Raman spectroscopy, *Journal of Raman Spectroscopy*, Vol. 44, Issue 7, 2013, pp. 1018-1021.

[28]. Y. Sun, M. Yanagisawa, T. Homma, Thermal stability of single-layer graphene subjected to confocal laser heating investigated by using in situ anti-Stokes and Stokes Raman spectroscopy, *Electrochemistry*, Vol. 85, Issue 4, 2017, pp. 195-198.
